Available online at www.sciencedirect.com
ScienceDirect
Ceramics International 35 (2009) 2809–2815
CERAMICS INTERNATIONAL
www.elsevier.com/locate/ceramint

Low-temperature synthesis of $La_{0.6}Sr_{0.4}Co_{0.2}Fe_{0.8}O_{3-\delta}$ perovskite powder via asymmetric sol–gel process and catalytic auto-combustion

Lei Ge [a], Ran Ran [a], Zongping Shao [a,**], Zhong Hua Zhu [b,*], Shaomin Liu [c]

[a] State Key Laboratory of Materials-oriented Chemical Engineering, College of Chemistry & Chemical Engineering, Nanjing University of Technology, Nanjing 210009, PR China
[b] Division of Chemical Engineering, The University of Queensland, Brisbane, Queensland 4072, Australia
[c] Department of Chemical Engineering, Curtin University of Technology, Perth, WA 6845, Australia

Received 25 January 2009; received in revised form 10 February 2009; accepted 15 March 2009
Available online 15 April 2009

Abstract

$La_{0.6}Sr_{0.4}Co_{0.2}Fe_{0.8}O_{3-\delta}$ powder was synthesized by a combined EDTA-citrate complexing process via low-temperature auto-combustion synthesis with NH_4NO_3 as an oxidizer and a combustion trigger. Two novel methods were explored to improve this auto-combustion technology with reduced NH_4NO_3 addition: the use of $La_{0.6}Sr_{0.4}Co_{0.2}Fe_{0.8}O_{3-\delta}$ as the combustion catalyst and the application of asymmetric sol–gel process to provide the precursor with different NH_4NO_3 concentrations. The prepared perovskite powder was characterized by BET, SEM, XRD and iodometric titration techniques. The catalytic performance of the powder was also examined in the decomposition of peroxide hydrogen. Experimental results indicate that powders from catalytic combustion and asymmetric precursor routes have more advantages in terms of better crystallites, higher specific surface area, higher B-site valence state, improved sintering capability and better catalytic performance in peroxide hydrogen decomposition than that from the synthesis with uniform NH_4NO_3 distribution.

Keywords: Ceramic powder; Auto-combustion synthesis; Asymmetry; Catalysis

1. Introduction

Oxygen ionic conducting perovskite oxides have attracted much attention from many academic or industrial researchers for their potential applications as oxygen selective membranes for air separation, catalytic membrane reactor for high temperature oxidations, gas partial oxidations and electrode catalyst for solid oxide fuel cells (SOFC) [1–5]. Since the early 1980s when Teraoka et al. [6,7] demonstrated that high oxygen permeation flux could be achieved from $SrCo_{0.8}Fe_{0.2}O_3$ perovskites, an increased interest has been generated to develop new perovskite membranes with improved phase stability and oxygen permeation flux by optimizing the metal oxide compositions in the perovskite structure with a general stoichiometric formula of $A_yA'_{(1-y)}B_xB'_{(1-x)}O_{(3-\alpha)}$. Recently, mixed conducting perovskites were also applied as cathode material for solid oxide fuel cells and exhibited excellent performance both in dual and single chamber configurations [8–11]. This further spurred the research interest of investigating these perovskites as promising materials for future energy saving and environmental conservation.

In general, applications of these ionic conducting perovskite materials always start with the synthesis of the corresponding ceramic powders, and the conventional solid state reaction route is often applied. In this method, the starting materials like carbonates or metal oxides, mixed in a stoichiometric ratio to yield the given composition, are ball-milled, ground and sintered at a high temperature [12]. Such a synthesis method often leads to the following disadvantages: (1) a micro-homogenous phase structure can hardly be obtained due to large and strongly bonded powder agglomerates; (2) contamination can hardly be avoided during milling and grinding, resulting in a detrimental effect on the material properties; and (3) the mechanically ground mixture requires prolonged calcination at high temperatures (usually >1200 °C), which is undesirable in the fabrication of dense fine-grained ceramics due to the

* Corresponding author. Tel.: +61 7 33653528; fax: +61 7 33653528.
** Corresponding author. Tel.: +86 25 83172256; fax: +86 25 83172256.
E-mail addresses: shaozp@njut.edu.cn (Z. Shao), z.zhu@uq.edu.au (Z.H. Zhu).

0272-8842/$36.00
doi:10.1016/j.ceramint.2009.03.018

promotion of abnormal crystallite growth. Consequently, both the electrical and mechanical properties of the final sintered ceramic products by the conventional standard method are not adequate for many advanced applications. In order to obtain homogeneous fine powders, other different methods via various wet-chemistry routes such as freeze-drying, co-precipitation and combustion of metal-organic precursors, have been proposed [13–22]. Among these techniques, the combustion method based on water-soluble chelated complexes as precursors to obtain the homogeneity of the metal ion distribution on the atomic level, is currently attracting considerable attention. Such a water-soluble complex precursor synthesis route has shown to be advantageous for obtaining carbonate-free, chemical homogeneous oxide compounds with a high relative density and a high bending strength [18–22].

In the previous paper, we systematically investigated the modified Pechini method to prepare perovskite powder having a composite composition of four metal oxides [17]. In that method, ethylenediaminetetraacetic acid (EDTA) and citric acid were jointly used as the chelating ligands and ammonium nitrate (NH_4NO_3) was introduced as the combustion aid for low-temperature synthesis [23]. Compared to the standard Pechini method, the synthesis with NH_4NO_3 addition not only eliminates one sintering step at high temperatures, but also shortens the synthesis time. However, some toxic gases like NO_x may be produced due to the usage of NH_4NO_3, unfavorable for environmental conservation. From the viewpoint of application, the addition of NH_4NO_3 should be also reduced to decrease the material cost. In this study, we further improved this technology by minimizing the addition of NH_4NO_3 via the asymmetric sol–gel technique and the use of the prepared perovskite itself as the catalyst to facilitate the auto-combustion. The concept of asymmetric sol–gel with different NH_4NO_3 concentration was firstly applied in the field. The powder properties, such as sintering ability, microstructure and its catalytic efficiency in the decomposition of hydrogen peroxide were examined. Perovskite $La_{0.6}Sr_{0.4}Co_{0.2}Fe_{0.8}O_{3-\delta}$ (LSCF) is selected for the target material of investigation.

2. Experimental

2.1. Powder preparation

Cobalt nitrate, ferric nitrate, lanthanum nitrate, and strontium nitrate, all in analytical grades, were used as the metal sources. EDTA powder and citric acid with purities higher than 99.5% were used as the chelants. The mole ratio of EDTA and citric acid to metal ions in this study was fixed at 1:2:1. EDTA powder was added into aqueous ammonium hydroxide to form a water-soluble ammonium salt. Stoichiometric amounts of metal nitrates were dissolved in distilled water. The required amount of EDTA, citric acid, and NH_4NO_3 for the preparation of 0.005 mol LSCF was introduced in sequence into the nitrate solution under stirring condition. The mixed solution was then heated at ~90 °C over a hot plate under magnetic stirring until a gel was formed, which was cooled down to room temperature and then transferred to a pre-heated oven at 250 °C for auto-combustion [23]. When LSCF was applied as the combustion catalyst during the synthesis, the well-crystallized LSCF powder derived from the normal EDTA-citrate method (sintered at 800 °C for 5 h) [17] was added into the mixed solution and heated with stirring to ensure the uniform dispersion in the formed gel. As shown in Fig. 1, three different types of the NH_4NO_3 distribution in the gel system were illustrated. The asymmetrical gels with different concentration of NH_4NO_3 in vertical direction were prepared by multi-steps of thickening the mixed solutions with different NH_4NO_3 concentration. The schematic diagram of the auto-combustion reactor is shown in Fig. 1, where *M* stands for the different molar ratios of NH_4NO_3 to metal ions in the mixed solution. The auto-combustion experiment was conducted within a 250 mL Pyrex beaker, which was put inside a 2 L beaker for security issue and powder collection. An electrical fan was used during the heat treatment to ensure a homogeneous temperature distribution, and also to enhance the gas flow inside the oven. After the auto-combustion synthesis, the resulted powders were pressed in a 15 mm-diameter die at ~200 MPa to form cylindrical disks, which were then heated at 1000 °C under static air for 5 h to observe the sintering behavior of the as-synthesized powders.

2.2. Characterization

The temperatures of the gels during auto-combustion were monitored by the thermocouple inserted inside the gel and the temperature–time profiles were recorded by Yudian 708P temperature indictors with Labview program with a sampling rate of ten points per second [23]. The crystal phase structure of the synthesized powders was determined by X-ray diffraction (XRD, Bruker D8 Advance) using Cu Kα radiation at room temperature by step scanning in the range of $10 \leq \theta \leq 90^{\circ}$. The weight loss profile of the samples was examined by the Thermal Gravity Analysis (TGA) using a NETZSCH STA 409 thermal gravity analyzer under flowing air atmosphere at the rate of

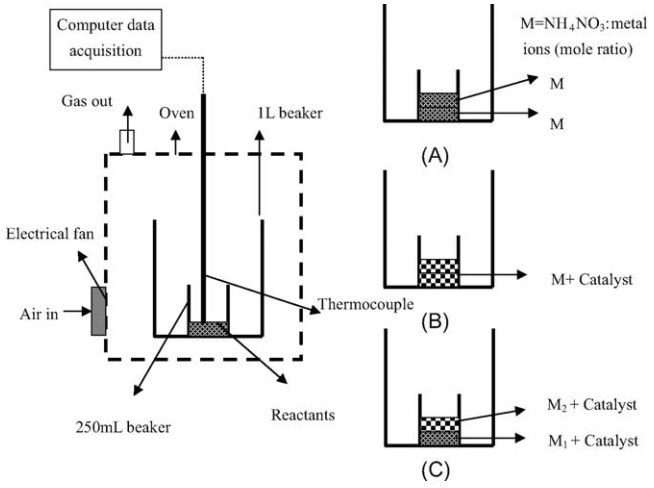

Fig. 1. Schematic diagram of the auto-combustion reactor and the NH_4NO_3 distribution in the gel system (precursor: (A) homogeneous NH_4NO_3 distribution, (B) LSCF catalyst addition, (C) asymmetric NH_4NO_3 distribution with LSCF catalyst).

10 mL/min. The specific surface area of the powders then obtained was characterized by N_2 adsorption using a BELSORP II instrument. Prior to the measurement, the samples were pre-treated at 200 °C for 2 h under vacuum to remove the surface adsorbed species. The morphologies of the sintered pellets or powders were examined using an Environmental Scanning Electron Microscopy (ESEM, QUANTA-2000).

The catalytic efficiency of the prepared perovskite powder was tested by decomposing the peroxide hydrogen. For this purpose, 7.5 mL H_2O_2 solution (0.2 mol/L) was added into 30 mL NaOH solution (6 mol/L) and 50 mg perovskite powder was subsequently added inside the reactant solution. The reaction rate was measured by the production rate of oxygen at room temperature (298 K). The hydrogen peroxide decomposition reaction can be expressed as [24]:

$$HO_{2(aq)}^{-} \rightarrow \frac{1}{2}O_2 + OH_{(aq)}^{-} \quad (1)$$

The B-site cation valence of as-prepared powder was measured by the iodometric titration technique [25]. Samples were dissolved in a solution of potassium iodide in HCl and heated in an oxygen-free environment. The iodide reduced the B-site ions of B^{3+} or B^{4+} to B^{2+} and was simultaneously oxidized to form I_2 which was quantified via redox titration with thiosulfate. The average B-site cation valence and oxygen vacancy stoichiometry were calculated based on the amount of I_2 formed.

3. Results and discussion

3.1. Auto-combustion synthesis with uniform NH_4NO_3 distribution

The combined EDTA-citrate complexing method is very effective to disperse metal ions in a molecular level in the resulted gel. No combustion was observed during the heat treatment of the gel up to 250 °C and subsequent sintering step at high temperatures is still needed to get the powder with desired perovskite structure [17]. With the addition of NH_4NO_3 as the combustion aid, the gel would go through the auto-combustion process in a heated environment around 250 °C. Fig. 2 shows the temperature–time profiles of the gels at various NH_4NO_3 additions when the auto-combustion started. Depending on the mole ratios of NH_4NO_3 to metal ions in the mixed solution (M), the combustion properties of the gels varied [23]. With the increase of NH_4NO_3 addition, the gel started the auto-combustion with gentle smothering type at $M = 9$ and transferred to self-propagating combustion at $M = 12$. The gel's combustion can also reach a higher flame temperature when more NH_4NO_3 was added. For example, the flame temperatures of the gels with M values of 9 and 12 can reach up to 300 and 500 °C, respectively. It is noteworthy that, in Fig. 2, the time for gel heating before gel bubbling varies with gel initial temperature and heating temperature, but not affected by the M value [23]. In this paper, the heating temperature was fixed at 250 °C, the gel heating time was mainly determined by gel initial temperature which rarely affects the peak temperature of auto-combustion. The research focus here is the peak temperature instead of the heating time. Fig. 3 displays the X-ray diffraction patterns of the powders after auto-combustion at different conditions. As can be seen, the development of LSCF perovskite crystalline phase from the precursor gel is a function of NH_4NO_3 content. When M is less than 9, most of the resultant powder is still in amorphous state. For $M \geq 9$, the perovskite phases starts to be formed. At a higher NH_4NO_3 content, the crystal phase patterns become more intense and the diffraction peaks reduce their widths gradually. It is interesting to note that no any intermediate phases were detectable in the samples after combustion no matter how the values of M changes. In order to guarantee that the LSCF perovskite structure is formed well, the NH_4NO_3 addition in the mixed solution for the preparation of LSCF powders kept at $M \geq 12$. In the following sections for the comparative studies of combustion properties from various precursors with LSCF catalyst addition or asymmetric NH_4NO_3 distribution were focused on these precursors with M values fixed at 9.

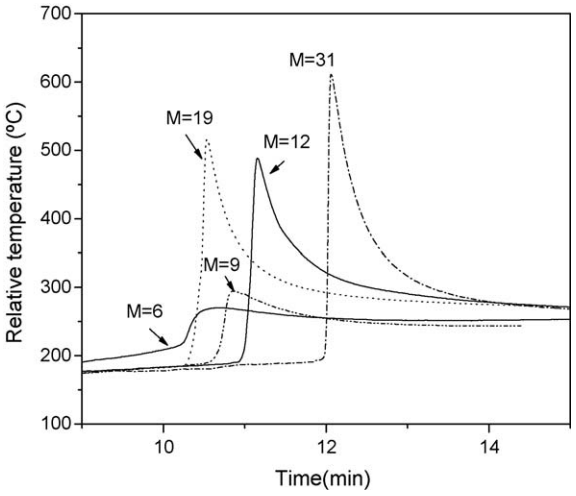

Fig. 2. Temperature–time profiles of the gels condensed from various NH_4NO_3 addition when the auto-combustion processes were started.

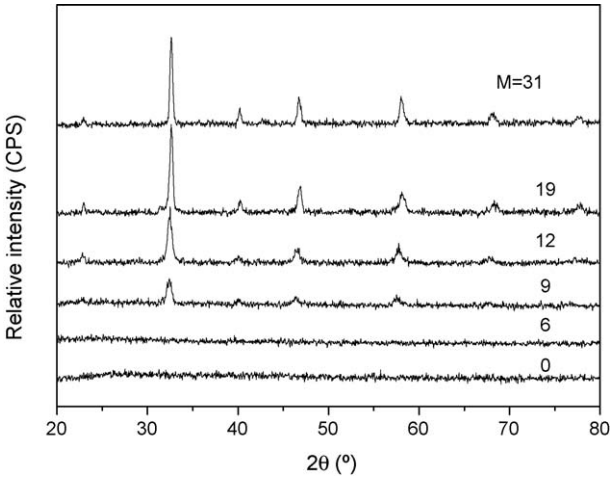

Fig. 3. XRD patterns of the powders after auto-combustion of the gels with different NH_4NO_3 contents.

3.2. The LSCF catalytic effects on the auto-combustion

In addition to the good materials for mixed conducting membranes and electrodes for solid oxide fuel cells, $LaCoO_3$-based perovskites can also be used as catalysts for combustion and the oxidizer (e.g. NH_4ClO_4) decomposition [26,27]. In this study, the well-crystallized LSCF powder was also tried as a combustion catalyst by dispersed uniformly in the precursor. During the combustion process, flame was clearly observed when LSCF catalyst was applied while only some sparks were seen from the slow smothering combustion without catalyst. Experimental results of the catalytic effects on the pyrolysis of NH_4NO_3 and its combustion are given in Fig. 4 where the LSCF catalyst loading in the gel is 10% by weight. Fig. 4a describes the thermal pyrolysis history recorded by TGA. Both samples of NH_4NO_3 with or without catalyst started to lose weight at 175 °C at which the decomposition of NH_4NO_3 is taking place. This intensive exothermic reaction will provide sufficient energy to trigger the auto-combustion. A big weight loss of the precursor without catalyst claimed about 95% in the range from 175 to 325 °C due to the complete decomposition of NH_4NO_3. The addition of LSCF catalyst accelerates the decomposition process and the big weight loss of the precursor was completed quickly in a shorter temperature range from 175 to 275 °C. This more intensive exothermic reaction will provide sufficient energy to trigger the subsequent precursor auto-combustion leading to less NH_4NO_3 addition.

Fig. 4b and c compare the temperature–time profiles and XRD results of the powders from the precursors ($M = 9$) with and without LSCF catalyst. Again, the flame in auto-combustion process with LSCF catalyst addition was clearly observed and higher flame peak temperature was achieved. Consequently, the as-prepared powder with better crystal structure is obtained due to the contribution of LSCF catalyst.

3.3. Auto-combustion synthesis with asymmetric precursor

In order to improve the combustion technology to produce perovskite powder with less use of NH_4NO_3, combustion behavior using the asymmetric precursor with various NH_4NO_3 concentrations in vertical orientation was further investigated. The basic idea is that the top layer with higher NH_4NO_3 content can trigger the combustion; once started, the combustion process will continue until the entire gel is burning out. The experimental work to verify this concept was conducted on three samples with results as shown in Fig. 5. Sample-I-gel with homogeneous NH_4NO_3 distribution ($M = 9$) and Sample-II-gel with different NH_4NO_3 distribution (top layer $M = 6$ and bottom layer $M = 12$) displayed invisible smothering combustion with lower flame peak temperatures ranged from 290 to 400 °C. Different to asymmetric Sample-II, Sample-III-gel with high NH_4NO_3 content on the top layer ($M = 12$) but lower concentration at the bottom layer ($M = 6$) has a self-propagating combustion and a highest flame peak temperature of 511 °C. As expected, the combustion from Sample-III-gel produced the perovskite powder with higher crystallinity due to the heat treatment at a higher flame temperature.

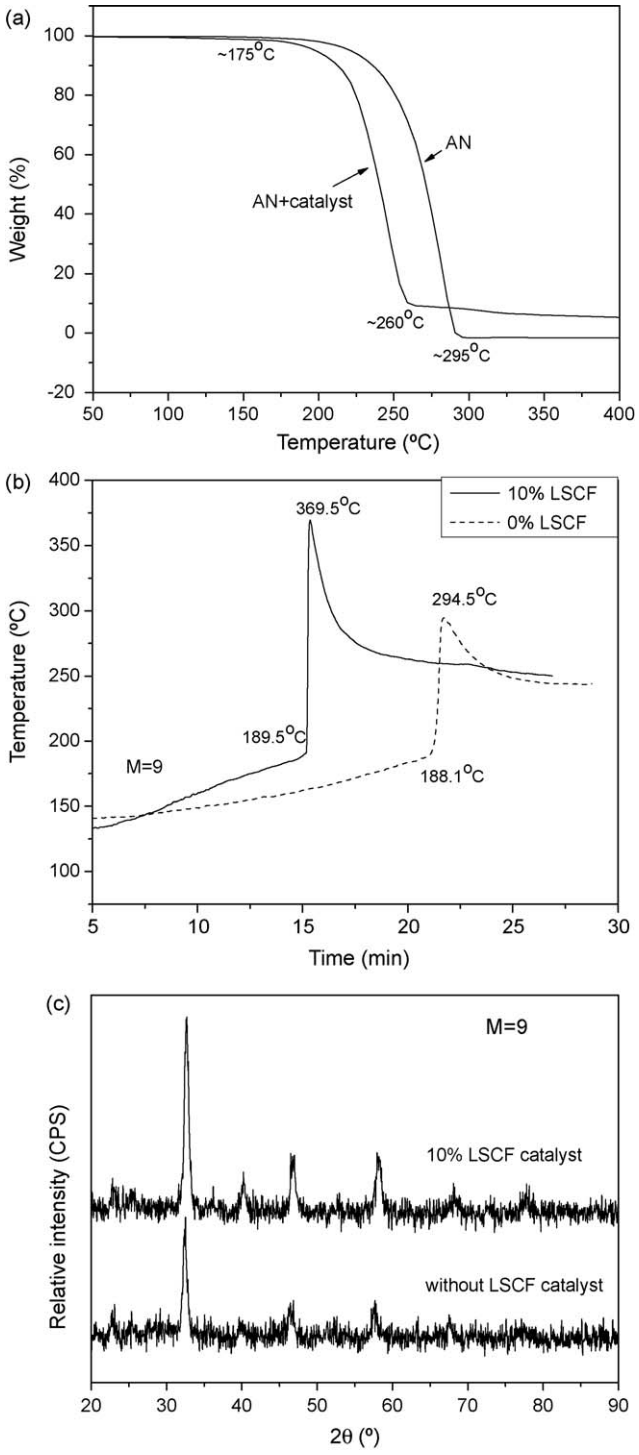

Fig. 4. TGA profiles of NH_4NO_3 with or without catalyst (a), flame temperature–time profiles (b) and XRD profiles (c) of the resulted powders for the precursor ($M = 9$) with various LSCF addition in the precursor as catalyst.

The larger NH_4NO_3 content in the top layer will release sufficient energy to ignite the precursor. The auto-combustion process requires a certain amount of oxygen, therefore the combustion of self-propagating type showed the wave-like flame from the top to the bottom of the burning media. It is important for the top layer to be ignited and then the

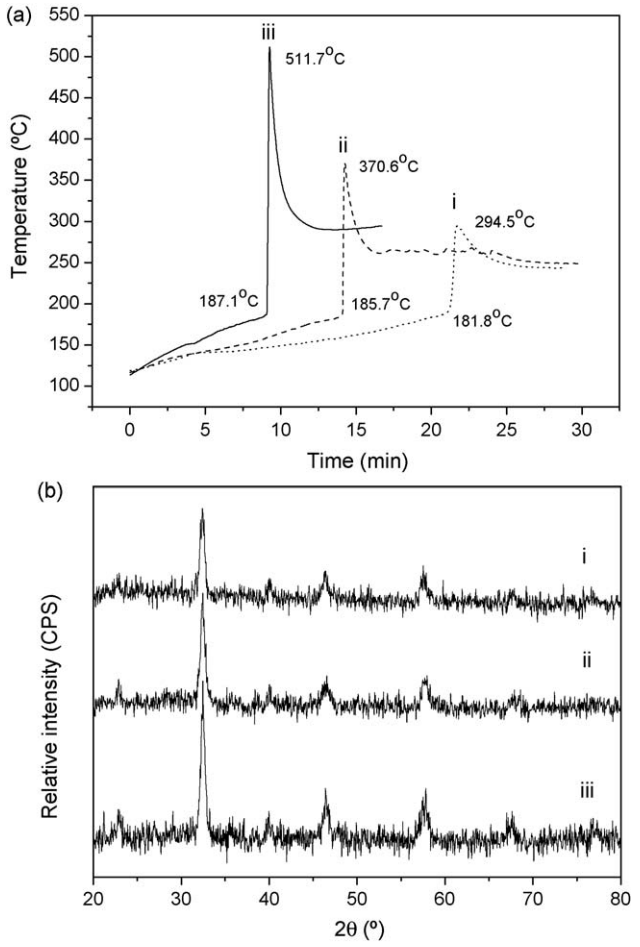

Fig. 5. Temperature–time profiles (a) and XRD profiles of the resulted powders at various gel composition (i: homogeneous NH_4NO_3 distribution with $M = 9$, ii: double layer, $M_1 = 6$ (top), $M_2 = 12$ (bottom), 10% LSCF catalyst; iii: double layer, $M_1 = 12$ (top), $M_2 = 6$ (bottom), 10% LSCF catalyst).

required heat and oxygen were transferred down to ignite the bottom layer with lower NH_4NO_3 amount. The top layer with higher NH_4NO_3 amount plays a vital role on triggering the combustion of the entire gel. On the contrary, in the case of Sample-II where a lower NH_4NO_3 amount was presented in the top layer and a higher NH_4NO_3 content in the bottom, the precursor lacks sufficient energy to reach the ignition point, and therefore cannot make a propagating combustion. Certainly, to make this method feasible for mass perovskite production, there is still a lot of work to optimize the NH_4NO_3 concentration gradient and the heating conditions including the temperature and the heating methods (e.g. microwave).

3.4. Powder and catalytic properties

Based on above discussion, the derived LSCF powders from three typical auto-combustion types (A: uniform NH_4NO_3 distribution, B: LSCF catalyst addition and C: asymmetric precursor synthesis) were further comparatively studied from their specific surface area, microstructure, sintering behavior and catalytic properties in peroxide hydrogen decomposition. Fig. 6 shows the SEM pictures of the as-prepared powders and their corresponding pellet membranes sintered from the powders. As shown in Fig. 6AI, method-A would produce larger, harder and denser powder agglomerates with specific surface area of 6.17 m^2/g, since its pyrolysis processes was sluggish and gases were released out slowly. Due to the faster pyrolysis and the higher flame temperatures, the powder agglomerates prepared by B and C methods have a more porous and sponge-like structure (Fig. 6BI and CI) with higher surface area of 11.56 and 12.75 m^2/g, respectively. It should be mentioned that these surface areas are quite comparable with that prepared by the typical EDTA-citrate complexing process and calcined at 600–900 °C for 5 h (5–20 m^2/g) [17]. Further inspection of the SEM pictures of the cross-sectional views of the sintered disk-shaped membranes reveals that many pores with size up to 20 microns exist inside the ceramics. The pore formation may be related to the carbon residue removal during the sintering process. The carbon is stemmed from the uncompleted organic burning during the combustion process. A careful examination of these porous structures indicates that ceramics of BII and CII have a more densified structure than that of AII. The better sintering capability of these perovskite powders derived from B and C methods is largely related to their cleaner perovskite phases with less carbon contamination due to the improved combustion with higher flame peak temperatures contributed from LSCF catalyst addition and asymmetric precursor preparation [23]. High sintering capability is very important for these perovskite powders to be applied as mixed conducting ceramic membrane materials for air separation as the membrane separating layer must fully densified to be gas tight for any molecular gases. It should be mentioned that the pores inside the ceramics B and C can be eliminated easily by carrying out sintering a higher temperature. Moreover, LSCF derived from methods B and C with self-propagating auto-combustion shows higher electrical conductivity and oxygen permeability than that derived from method-A with insufficient combustion model [28].

Catalytic activity of a catalyst is influenced by the preparation methods. The catalytic activity of powders derived from different combustion models was examined by the decomposition of peroxide hydrogen. The typical reaction profiles of time dependence of oxygen production are shown in Fig. 7. Obviously, compared with the powder from homogeneous NH_4NO_3 distribution (A), the decomposition rates of peroxide hydrogen were significantly improved for that of powders derived by LSCF catalysis (B) and asymmetric precursor fabrication (C).

For peroxide hydrogen decomposition, two of the most important factors which should be considered are: surface area and surface concentrations of active sites. For ABO_3 perovskite, the active sites are related to the valence state of B-site cations. In case of $A_yA'_{(1-y)}B_xB'_{(1-x)}O_{(3-\alpha)}$ with transition metals in the form of various B-site cation valences (B^{4+}, B^{3+} and B^{2+}), highly oxidized transition metal sites will increase the

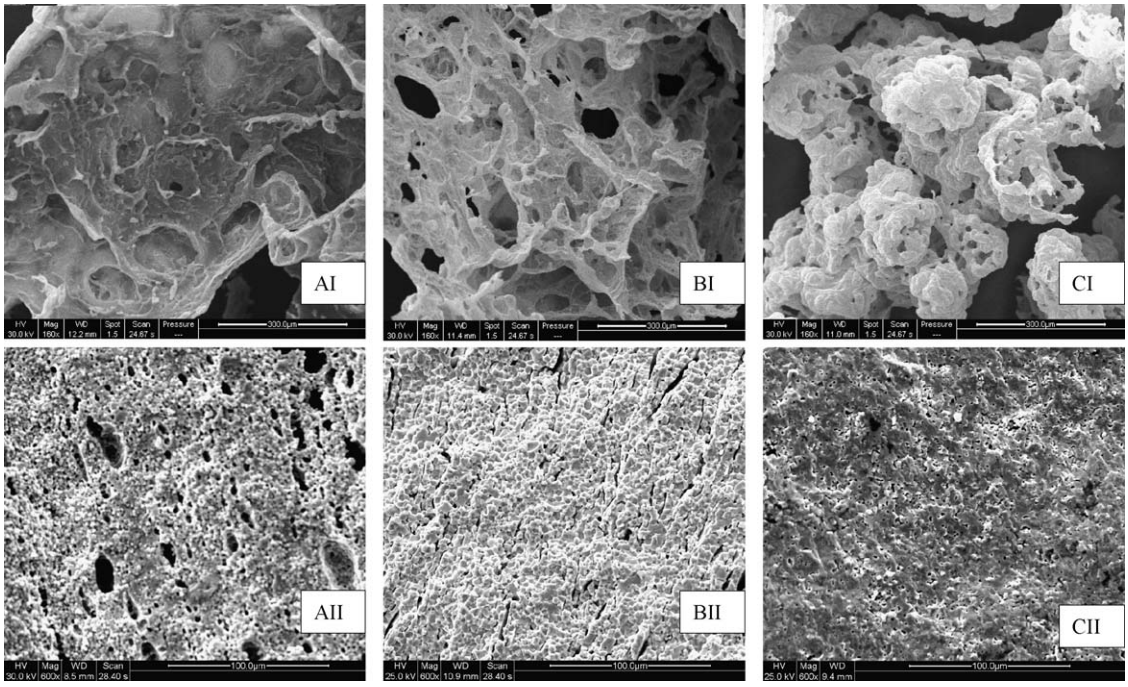

Fig. 6. SEM pictures of the as-prepared LSCF powders (I) and the sintered ceramic pellets (II) (A: homogeneous NH_4NO_3 distribution with $M = 9$, B: $M = 9$, with 10% LSCF catalyst addition; C: $M_1 = 12$ (top), $M_2 = 6$ (bottom), 10% LSCF catalyst) (pellets sintered at 1000 °C).

number of active constituents involved in the catalytic decomposition of H_2O_2 [29–31]. In this work, the iodometric titration method was employed to assess the B-site cation average valences of $La_{0.6}Sr_{0.4}Co_{0.2}Fe_{0.8}O_{3-\delta}$ at room temperature for both samples under air atmosphere. Results indicate that the average B-site cation valences for the powders prepared by three methods are 3.34 (method-A), 3.45 (method-B) and 3.47 (method-C), respectively. Due to the much larger surface areas and higher B-site valence state of the powders from method-B and C than that from method-A, it is reasonable to see that samples from B and C methods showed much higher catalytic activity.

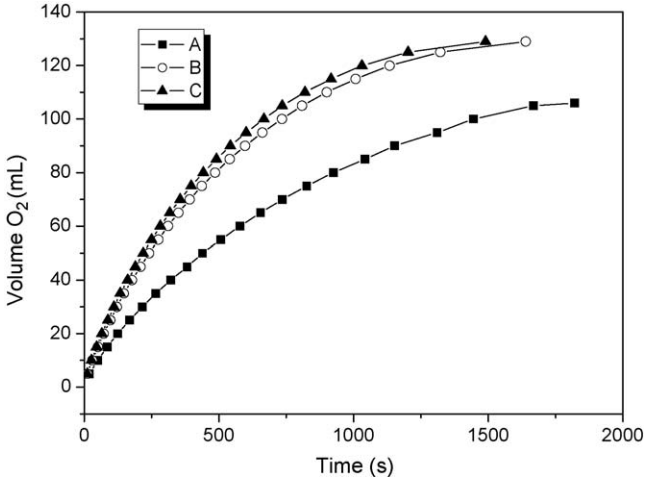

Fig. 7. The volumes of oxygen produced in the hydrogen peroxide decomposition as function of time (second) in the presence of different LSCF powders derived from different combustion synthesis methods (A: homogeneous NH_4NO_3 distribution with $M = 9$, B: $M = 9$, with 10% LSCF catalyst addition; C: asymmetric precursor, $M_1 = 12$ (top), $M_2 = 6$ (bottom), 10% LSCF catalyst).

4. Conclusions

$La_{0.6}Sr_{0.4}Co_{0.2}Fe_{0.8}O_{3-\delta}$ powder was synthesized by a combined EDTA-citrate complexing process via low-temperature auto-combustion synthesis with NH_4NO_3 as an oxidizer and a combustion trigger. The as-prepared pure LSCF powder itself can be used as a catalyst to facilitate the auto-combustion and to improve the powder properties. In order to further reduce the NH_4NO_3 addition, the concept of asymmetric sol–gel was also applied to provide the precursor powder with various concentrations of NH_4NO_3 in vertical orientation. With these novel methods, LSCF powder can be synthesized via low-temperature auto-combustion with better crystallites, higher specific surface area, higher B-site valence state, improved sintering capability and better catalytic performance in peroxide hydrogen decomposition. In view of its simplicity and many unique features, we expect that the present methods would be useful for providing an alternative of low cost mass production of perovskite powders.

Acknowledgements

This work was supported by the National Natural Science Foundation of China under contract Nos. 20676061, 20703024 and 20701020, by the National 863 program under contract No. 2007AA05Z133, and by the National Basic Research Program of China under contract No. 2007CB209704. The financial support from the Australian Research Council discovery project is also greatly appreciated.

References

[1] H.J.M. Bouwmeester, A.J. Burggraaf, Dense ceramic membranes for oxygen separation, in: A.J. Burggraaf, L. Cot (Eds.), Fundamentals of Inorganic Membrane Science and Technology, Elsevier, Amsterdam, 1996, p. 435.

[2] Y.S. Lin, Y. Zeng, Catalytic properties of oxygen semipermeable perovskite-type ceramic membrane materials for oxidative coupling of methane, J. Catal. 164 (1996) 220–231.

[3] J.E. ten Elshof, H.J.M. Bouwmeester, H. Verweij, Oxidative coupling of methane in a mixed-conducting perovskite membrane reactor, Appl. Catal. A 130 (1995) 195–212.

[4] S.P.S. Badwal, F.T. Ciacchi, Ceramic membrane technologies for oxygen separation, Adv. Mater. 13 (2001) 993–996.

[5] Z.P. Shao, S.M. Haile, A high-performance cathode for the next generation of solid-oxide fuel cells, Nature 431 (2004) 170–173.

[6] Y. Teraoka, H. Zhang, S. Furukawa, N. Yamazoe, Oxygen permeation through perovskite-type oxides, Chem. Lett. 11 (1985) 1743–1746.

[7] Y. Teraoka, H. Zhang, K. Okamoto, N. Yamazoe, Mixed ionic-electronic conductivity of $La_{1-x}Sr_xCo_{1-y}Fe_yO_{3-d}$, Mater. Res. Bull. 23 (1988) 51–58.

[8] A. Petric, P. Huang, F. Tietz, Evaluation of La–Sr–Co–Fe–O perovskites for solid oxide fuel cells and gas separation membranes, Solid State Ionics 135 (2000) 719–725.

[9] T. Hibino, A. Hashinmoto, T. Inoue, J. Tokuno, S. Yoshida, M. Sano, A low operating-temperature solid oxide fuel cell in hydrocarbon-air mixtures, Science 288 (2000) 2031–2033.

[10] N.P. Brandon, S. Skinner, B.C.H. Steele, Recent advances in materials for fuel cells, Annu. Rev. Mater. Res. 33 (2003) 183–213.

[11] Z.P. Shao, S.M. Haile, J. Ahn, P.D. Ronney, Z.L. Zhan, S.A. Barnett, A thermally self-sustained micro solid-oxide fuel-cell stack with high power density, Nature 435 (2005) 795–798.

[12] B.L. Cushing, V.L. Kolesnichenko, C.J. O'Connor, Recent advances in the liquid-phase syntheses of inorganic nanoparticles, Chem. Rev. 104 (2004) 3893–3946.

[13] M.P. Pechini, U.S. Patent 3,330,697 (1967).

[14] J. Sunarso, S. Baumann, J.M. Serra, W.A. Meulenberg, S. Liu, Y.S. Lin, J.C. Diniz da Costa, Mixed ionic–electronic conducting (MIEC) ceramic-based membranes for oxygen separation, J. Membr. Sci. 320 (2008) 13–41.

[15] A. Kwiatkowski, K. Reszka, A. Szymanski, Preparation of corundum and steatite ceramics by the freeze-drying method, Ceram. Int. 11 (1985) 143.

[16] S.P. Gaikwad, H.S. Potdar, V. Violet Samuel, Ravi, Co-precipitation method for the preparation of fine ferroelectric $BaBi_2Nb_2O_9$, Ceram. Int. 31 (2005) 379–381.

[17] W. Zhou, Z.P. Shao, W.Q. Jin, Synthesis of nanocrystalline conducting composite oxides based on a non-ion selective combined complexing process for functional applications, J. Alloy. Compd. 426 (2006) 368–374.

[18] K.A. Singh, L.C. Pathak, S.K. Roy, Effect of citric acid on the synthesis of nano-crystalline yttria stabilized zirconia powders by nitrate-citrate process, Ceram. Int. 33 (8) (2007) 1463–1468.

[19] G. Fagherazzi, S. Polizzi, M. Bettinelli, A. Speghini, Yttria-based nanosized powders: a new class of fractal materials obtained by combustion synthesis, J. Mater. Res. 15 (2000) 586–589.

[20] D.G. Lamas, R.E. Juarez, G.E. Lascalea, N.E.W. de Reca, Synthesis of compositionally homogeneous, nanocrystalline ZrO_2-35 mol% CeO_2 powders by gel-combustion, J. Mater. Sci. Lett. 20 (2001) 1447–1449.

[21] Y.B. Xu, X. Yuan, P.X. Lu, G.H. Huang, C.L. Zeng, Synthesis of $La(Mg_{1/2}Ti_{1/2})O_3$ powder through ethylenediaminetetraacetic acid gel combustion, Ceram. Int. 32 (1) (2006) 57–60.

[22] W. Zhou, Z.P. Shao, R. Ran, W.Q. Jin, N.P. Xu, Functional nanocomposite oxides synthesized by environmental-friendly auto-combustion within a micro-bioreactor, Mater. Res. Bull. 43 (8–9) (2008) 2248–2259.

[23] L. Ge, W. Zhou, R. Ran, Z.P. Shao, S.M. Liu, Facile auto-combustion synthesis of $La_{0.6}Sr_{0.4}Co_{0.2}Fe_{0.8}O_{3-\delta}$ (LSCF) perovskite via a modified complexing sol–gel process with NH_4NO_3 as combustion aid, J. Alloy. Compd. 450 (2008) 323–329.

[24] S.P. Jiang, Z.G. Lin, A.C. Tseung, Homogeneous and heterogeneous catalytic reactions in cobalt oxide/graphite air electrodes. I. Chemical kinetics of peroxide decomposition by Co(II) ions in alkaline solutions, J. Electrochem. Soc. 137 (3) (1990) 759–764.

[25] P.Y. Zeng, Z.H. Chen, W. Zhou, H.X. Gu, Z.P. Shao, S.M. Liu, Re-evaluation of $Ba_{0.5}Sr_{0.5}Co_{0.8}Fe_{0.2}O_{3-\delta}$ perovskite as oxygen semi-permeable membrane, J. Membr. Sci. 291 (2007) 148–156.

[26] Y.P. Wang, X.J. Yang, L.D. Lu, X. Wang, Experimental study on preparation of $LaMO_3$ (M = Fe, Co, Ni) nanocrystals and their catalytic activity, Thermochim. Acta 443 (2006) 225–230.

[27] M. Alifanti, J. Kirchnerova, B. Delmon, D. Klvana, Methane and propane combustion over lanthanum transition-metal perovskites: role of oxygen mobility, Appl. Catal. A: Gen. 262 (2004) 167–176.

[28] L. Ge, R. Ran, W. Zhou, Z.P. Shao, S.M. Liu, W.Q. Jin, N.P. Xu, Facile auto-combustion synthesis for oxygen separation membrane application, J. Membr. Sci. 329 (2009) 219–227.

[29] A. Ariafard, H.R. Aghabozorg, F. Salehirad, Hydrogen peroxide decomposition over $La_{0.9}Sr_{0.1}Ni_{1-x}Cr_xO_3$ perovskites, Catal. Commun. 4 (2003) 561–566.

[30] H. Falcón, R.E. Carbonio, J.L.G. Fierro, Correlation of oxidation states in $LaFe_xNi_{1-x}O_{3+\delta}$ oxides with catalytic activity for H_2O_2 decomposition, J. Catal. 203 (2001) 264–272.

[31] N.A.M. Deraz, Catalytic decomposition of H_2O_2 on promoted cobaltic oxide catalysts, Mater. Lett. 57 (2002) 914–920.